

## Article

# Proteolytic cleavage is required for functional neuroligin 2 maturation and trafficking in *Drosophila*

Renjun Tu<sup>1</sup>, Jinjun Qian<sup>1</sup>, Menglong Rui<sup>2</sup>, Nana Tao<sup>1</sup>, Mingkuan Sun<sup>2</sup>, Yan Zhuang<sup>2</sup>, Huihui Lv<sup>1</sup>, Junhai Han<sup>1,2</sup>, Moyi Li<sup>1,2</sup>, and Wei Xie<sup>1,2,\*</sup>

<sup>1</sup> Institute of Life Sciences, The Collaborative Innovation Center for Brain Science, Southeast University, 2 SiPaiLou Road, Nanjing 210096, China

<sup>2</sup> The Key Laboratory of Developmental Genes and Human Disease, Jiangsu Co-innovation Center of Neuroregeneration, Southeast University, 2 SiPaiLou Road, Nanjing 210096, China

\* Correspondence to: Wei Xie, E-mail: wei.xie@seu.edu.cn

**Neuroligins (NLGs) are transmembrane cell adhesion molecules playing essential roles in synapse development and function. Genetic mutations in *neuroligin* genes have been linked with some neurodevelopmental disorders such as autism. These mutated NLGs are mostly retained in the endoplasmic reticulum (ER). However, the mechanisms underlying normal NLG maturation and trafficking have remained largely unknown. Here, we found that *Drosophila* neuroligin 2 (DNlg2) undergoes proteolytic cleavage in the ER in a variety of *Drosophila* tissues throughout developmental stages. A region encompassing Y642–T698 is required for this process. The immature non-cleavable DNlg2 is retained in the ER and non-functional. The C-terminal fragment of DNlg2 instead of the full-length or non-cleavable DNlg2 is able to rescue neuromuscular junction defects and GluRIIB reduction induced by *dnlg2* deletion. Intriguingly, the autism-associated R598C mutation in DNlg2 leads to similar marked defects in DNlg2 proteolytic process and ER export, revealing a potential role of the improper NLG cleavage in autism pathogenesis. Collectively, our findings uncover a specific mechanism that controls DNlg2 maturation and trafficking via proteolytic cleavage in the ER, suggesting that the perturbed proteolytic cleavage of NLGs likely contributes to autism disorder.**

**Keywords:** neuroligin, proteolytic cleavage, maturation, trafficking, autism

## Introduction

Synapses are asymmetric intercellular junctions communicating with different neurons. These junctions are basal units required to establish neuronal networks for normal nervous system function. They are composed of presynaptic and postsynaptic areas that are consisted of many adhesion molecules (Giagtzoglou et al., 2009). Among synaptic adhesion molecules, neuroligins (NLGs) are postsynaptic single transmembrane proteins with an extracellular domain that exhibits homology to acetylcholinesterase (AChE) (Ichtchenko et al., 1995). NLGs and their binding partners neuroligins (Nrxs) form heterophilic adhesive complexes via an extracellular  $\alpha/\beta$  hydrolase fold domain

(Südhof, 2008). NLGs can organize presynaptic and postsynaptic structures and are essential for synapse development and synaptic transmission (Knight et al., 2011). The intracellular region of NLGs can interact with several postsynaptic molecules, which are thought to recruit postsynaptic proteins to synaptic sites, such as PSD-95 (Irie et al., 1997).

Mutations in human NLGs have been found to be associated with autism and other neurodevelopmental impairments, e.g. the R451C mutation in NLG3 and the R87W mutation in NLG4 (Jamain et al., 2003; Szatmari et al., 2007; Jiang, 2015). These mutations give rise to defects in protein folding and trafficking (De Jaco et al., 2010). R451C mutation in NLG3 leads to activation of the unfolded protein response (Ulbrich et al., 2016) and also differentially alters hippocampal and cortical synaptic function (Eherton et al., 2011). However, the precise mechanisms by which these mutations give rise to defects in NLG functions remain unclear. It is likely that aberrant protein maturation process and mislocalization of mutant NLGs contribute to their potential pathogenesis. Whether the autism-associated mutation affects the proteolytic cleavages of NLGs are still mysteries.

Received October 26, 2016. Revised December 20, 2016. Accepted May 3, 2017.

© The Author (2017). Published by Oxford University Press on behalf of *Journal of Molecular Cell Biology*, IBCB, SIBS, CAS.

This is an Open Access article distributed under the terms of the Creative Commons Attribution Non-Commercial License (<http://creativecommons.org/licenses/by-nc/4.0/>), which permits non-commercial re-use, distribution, and reproduction in any medium, provided the original work is properly cited. For commercial re-use, please contact journals.permissions@oup.com

One crucial biological process regulating protein maturation, trafficking, and activity is proteolytic cleavage. It is universally involved in various biological events such as cell signaling, development, and apoptosis (Vogel and Kristie, 2000). Unlike protein precursors usually cleaved in the endoplasmic reticulum (ER) or Golgi, Nlgs display strong tendency of local proteolytic process based on current findings. Rodent Nlg1 undergoes activity-dependent proteolytic cleavage by ADAM10/MMP9 on synapses, which may negatively regulate synapse remodeling (Peixoto et al., 2012; Suzuki et al., 2012). While the N-terminal ectodomain is secreted to the outside of the cell membrane, Nlg1 C-terminal fragment (CTF) is subsequently cleaved by presenilin/ $\gamma$ -secretase (Suzuki et al., 2012). These further cleaved CTFs regulate spine dynamics and synaptic plasticity via LIMK1/cofilin-mediated actin reorganization (Liu et al., 2016). The secreted N-terminal fragments (NTFs) of Nlg3 promote robust glioma cell proliferation via PI3K–mTOR pathway (Venkatesh et al., 2015), suggesting that Nlg3 proteins also undergo proteolytic cleavage. The AChE, a homology to Nlg extracellular domain, also undergoes proteolytic cleavage playing important roles in apoptosis (Xie et al., 2011). Collectively, post-translational proteolytic cleavages are common modifications in protein maturation and function. Therefore, whether the proteolytic cleavage modification is involved in Nlg maturation and trafficking is urgent to be determined.

Intriguingly, Nlgs with less molecular weight can be detected in *Drosophila* as well. Among four Nlg homologs in *Drosophila*, *Drosophila* neuroligin 2 (DNlg2) and DNlg3 have both full-length and partial-length forms (Banovic et al., 2010; Sun et al., 2011; Mozer and Sandstrom, 2012; Hahn et al., 2013; Li et al., 2013; Xing et al., 2014; Qian et al., 2016). However, the mechanisms of their protein processing events and the function of partial-length proteins have yet to be determined. It is very important to verify whether the cleavage mechanisms and functions of other Nlgs are similar or specific.

In this study, we demonstrate that, different from rodent Nlgs, DNlg2 is cleaved in the ER rather than in the synapse cleft. This protein processing event is necessary for its maturation and trafficking. Cleavage of DNlg2 is ubiquitous in *Drosophila* and occurs throughout development. The full-length DNlg2 proteins are immature and retained in the ER through the association with the ER chaperon protein BIP. Mature CTF but not full-length DNlg2 proteins locate at synapse and promote synapse development. Interestingly, we also found that autism-associated R598C mutation leads to severe defects in DNlg2 cleavage and trafficking. Together, our results indicate a significant advancement in understanding the diverse mechanisms and functions of Nlg proteolytic cleavage and suggest a potential autism pathogenesis.

## Results

### *DNlg2 is ubiquitously cleaved*

Previous study reported that only 4.8-kb *dnlg2* mRNA was detected in wild-type (WT) flies, which was predicted to give rise to 130 kDa full-length proteins (Sun et al., 2011). However, in our immunoblotting analysis, the predominant band observed was 70 kDa (Sun et al., 2011). Immunoprecipitation experiment showed

that endogenous 130 kDa DNlg2 proteins really existed in WT flies at very low level compared with the 70 kDa DNlg2 (Supplementary Figure S1A). In addition, three *neurexin* genes have been identified in mammalian, each encoding a longer  $\alpha$ -Nrx and a shorter  $\beta$ -Nrx by independent promoters (Südhof, 2008). Therefore, we first investigated whether the 70 kDa DNlg2 is cleaved from the full-length DNlg2 or encoded from another promoter.

Site-directed *UAS-dnlg2* transgene was generated using the  $\varphi$ 31-mediated integration system (Bischof et al., 2007). We took the advantage of the *Gal4/Tub-Gal80<sup>ts</sup>* system, which allows temperature inducible activation of gene expression. At the permissive temperature (25°C), binding of *Gal80<sup>ts</sup>* to *Gal4* prevents the transcription of DNlg2 (Supplementary Figure S1B). After shifting to 30°C, *Gal80<sup>ts</sup>* was inactivated, allowing *Gal4* to activate the transcription of *dnlg2*, which was then translated into DNlg2 protein (Supplementary Figure S1B). Immunoblotting results showed that the 130 kDa DNlg2 was detected earlier than the 70 kDa DNlg2 (Figure 1A). And the signal of 130 kDa DNlg2 was also stronger than that of the 70 kDa DNlg2 after 24–37 h incubation at 30°C (Figure 1A). After incubation at 25°C for 9 h, a dramatic reduction in the expression of the 130 kDa DNlg2 and a concomitant increase in the level of the 70 kDa DNlg2 were observed (Figure 1A). These results indicate that the 70 kDa DNlg2 is cleaved from the 130 kDa DNlg2. The fact that the 70 kDa DNlg2 was detected nearly 16 h later than the 130 kDa DNlg2 indicates that the cleavage of DNlg2 could be a slow process (Figure 1A).

We next asked whether the 70 kDa DNlg2 is expressed in all developmental stages of WT flies. Interestingly, immunoblotting results showed that from embryonic stage to adult stage, only the 70 kDa DNlg2 can be constantly detected (Figure 1B). These results suggest that the 70 kDa DNlg2 is the predominant form existing in all *Drosophila* developmental stages.

We also investigated the tissue specificities of the 70 kDa DNlg2. Using the *UAS/Gal4* system, *dnlg2* cDNA was expressed specifically in neurons with *elav-Gal4*, in all cells with *da-Gal4*, in eyes with *gmr-Gal4*, or in glial cells with *repo-Gal4*. We performed immunoblotting analysis and found that DNlg2 was expressed and cleaved in all these tissues with similar ratios (Figure 1C). DNlg2 was overexpressed in S2 cells by transient transfection with a *pAc5.1/V5-His-A-dnlg2* plasmid. We found that the 70 kDa DNlg2 also existed in DNlg2-overexpressing S2 cells (Figure 1D). These observations indicate that the 70 kDa DNlg2 generally exists in various kinds of cells when DNlg2 is overexpressed.

### *DNlg2 cleavage is not an automatic reaction*

To further investigate whether the cleavage of DNlg2 is a specific event mediated by protease in *Drosophila* or just an automatic cleavage event, we tested the influence of protease inhibitor (PI) cocktail on DNlg2 cleavage. DNlg2 was expressed with the *Gal4/Tub-Gal80<sup>ts</sup>* system. After 37 h at 30°C, third instar larval muscle cells were dissected and treated with or without PI for 6 or 12 h in cell culture medium. Immunoblotting results showed that without PI, the level of the 70 kDa DNlg2 was increased, while the level of the 130 kDa DNlg2 was decreased after 6 or 12 h (Figure 1E). However, when treated

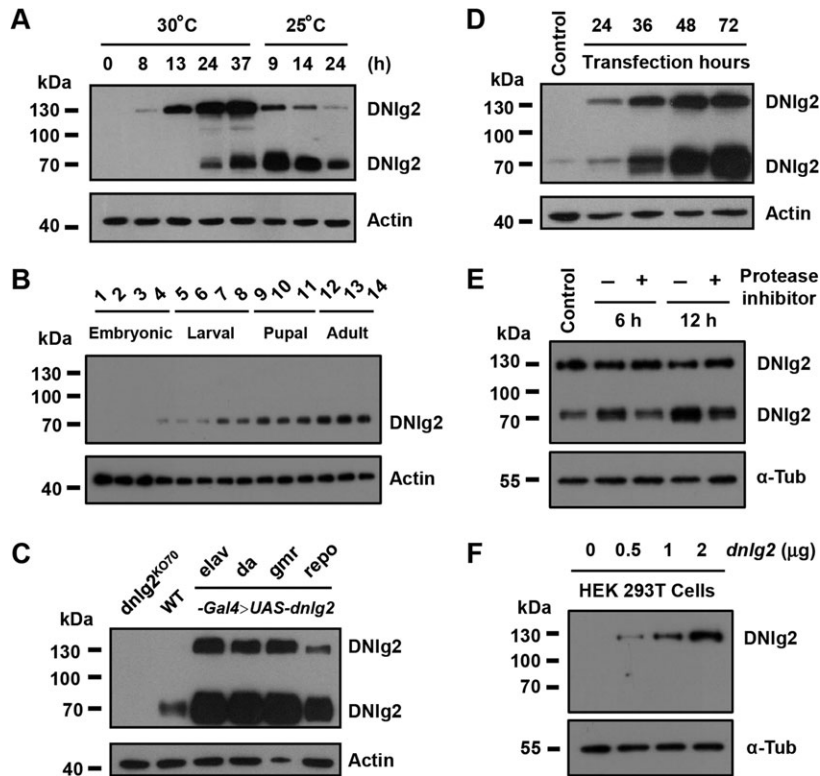


**Figure 1** Proteolytic cleavage of DNlg2. **(A)** Immunoblotting analysis of *Gal4/Tub-Gal80<sup>ts</sup>*-controlled DNlg2-overexpressing muscle cells. Entrainment temperature and incubated time (h) are shown at the top. **(B)** Immunoblotting analysis of WT *Drosophila* samples at different developmental stages (1–4: embryonic 0–6 h, 6–12 h, 12–18 h, 18–24 h; 5–8: larval of 1st, 2nd, early 3rd, late 3rd instar; 9–11: pupal head after 24, 48, 72 h pupation; 12–14: adult head 1 day, 3 days, 5 days). **(C)** Immunoblotting analysis of *dnlg2* mutant, WT, *elav-Gal4 > UAS-dnlg2*, *da-Gal4 > UAS-dnlg2*, *gmr-Gal4 > UAS-dnlg2*, and *repo-Gal4 > UAS-dnlg2* fly heads. **(D)** Immunoblotting analysis of S2 cells transfected with *pAc5.1-dnlg2* plasmid after 24, 36, 48, or 72 h. **(E)** Immunoblotting analysis of protease inhibitor (PI)-treated samples. DNlg2 proteins were overexpressed with the *Gal4/Tub-Gal80<sup>ts</sup>* expression system for 37 h. Then dissected muscle cells were incubated at 25°C with or without PI cocktail for 6 or 12 h. **(F)** Immunoblotting analysis of human 293T cells transfected with 0, 0.5, 1, or 2  $\mu$ g *pcDNA3.1-dnlg2* plasmid. The rabbit anti-DNlg2<sup>CTF</sup> antibodies were used.

with PI, both 70 kDa and 130 kDa protein levels did not markedly change compared with control (Figure 1E). This means that PI suppresses DNlg2 cleavage efficiently. Only the 130 kDa DNlg2 could be detected when DNlg2 was overexpressed in human 293T, human SH-SY5Y, or mouse Neuro-2A cells by transient transfection with *pcDNA3.1-dnlg2* plasmids (Figure 1F and Supplementary Figure S1C), indicating that DNlg2 is not cleaved in non-*Drosophila* cells.

Meanwhile, we examined whether DNlg2 can be self-cleaved *in vitro*. DNlg2 was expressed with the *Gal4/Tub-Gal80<sup>ts</sup>* system and was immunoprecipitated from third instar larval muscle cells after 37 h. The purified DNlg2 was treated with the buffer suitable for *in vitro* self-cleavage (Lin et al., 2004). At various time points, samples were withdrawn and analyzed by immunoblotting. We found that ratios of the 70 kDa DNlg2 to the 130 kDa DNlg2 were similar during 0–48 h of incubation (Supplementary Figure S1D). Taken together, these observations demonstrated that the cleavage of DNlg2 is not an autoproteolytic process but rather a specific *Drosophila* protease(s)-dependent event.

#### Proteolytic cleavage of DNlg2 is achieved in the ER

To unveil the proteolytic mechanism of DNlg2, we determined the subcellular component in which the cleavage takes place. Previous experiments have shown that the cleavage of mammal Nlg1 occurs at neural cell surface (Suzuki et al., 2012). Thus, we first examined whether the 130 kDa DNlg2 could locate on cell surface. A plasma membrane extraction kit was used to purify the plasma membrane proteins from whole-cell lysates of WT or DNlg2-overexpressing fly heads. Immunoblotting results showed that only the 70 kDa DNlg2 could be detected in the plasma fractions (Figure 2A). This means that most of the 130 kDa proteins are present in cytoplasm but not on plasma membrane. In addition, two intracellular proteins Fmr1 and  $\alpha$ -Tubulin were used as negative controls that were unable to be detected in plasma membrane fractions (Figure 2A). These observations indicate that the 130 kDa DNlg2 cannot locate on cell surface, and, therefore, the cleavage may be an intracellular reaction.

In order to identify the proposed intracellular organelles that responsible for DNlg2 cleavage, the ER and Golgi fractions were separated by using an ER isolation kit. Intracellular organelle

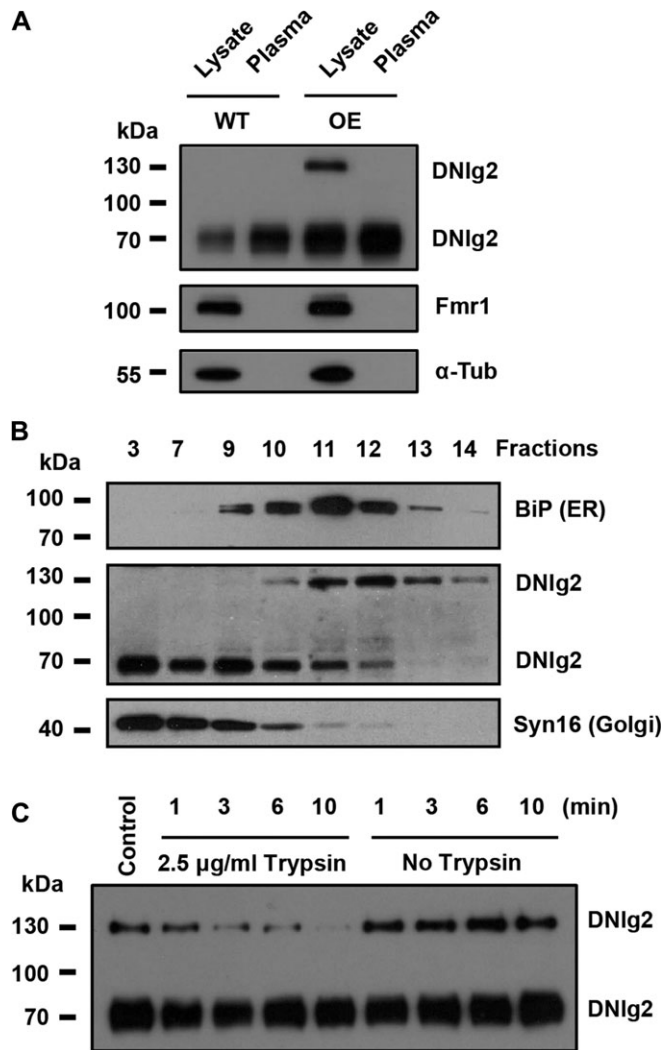


**Figure 2** Proteolytic cleavage of DNLg2 occurs in the ER. **(A)** Immunoblotting analysis of samples collected from purified plasma membrane fractions. Blots were probed with antibodies against DNLg2, Fmr1, and  $\alpha$ -Tubulin. Lysate means whole-cell fractions. Plasma means purified plasma membrane fractions. OE means DNLg2-overexpressing cells. **(B)** Immunoblotting analysis of samples collected from a 10%–30% density gradient separation prepared from adult WT heads. Blots were probed with antibodies against DNLg2 intracellular domain, the Golgi protein Syn16, and the ER protein BiP. **(C)** DNLg2 proteins were overexpressed and immunoprecipitated, and then digested with or without 2.5  $\mu$ g/ml trypsin for 1, 3, 6, or 10 min. Samples were then followed by immunoblotting with anti-DNLg2 antibody. The rabbit anti-DNLg2<sup>CTF</sup> antibodies were used.

fractions were extracted from a 10%–30% density gradient separation prepared from adult WT heads and subjected to immunoblotting with antibodies against the Golgi protein Syn16 (Xu et al., 2002), the ER protein BiP (Stein et al., 2010), and the DNLg2<sup>CTF</sup>, respectively. The 130 kDa DNLg2 was found to co-fractionate with BiP, while the 70 kDa DNLg2 was co-fractionated with both BiP and Syn16 (Figure 2B). These results strongly suggest that DNLg2 is cleaved in the ER and then delivered to Golgi as the 70 kDa isoform.

To further confirm the cleavage reaction of DNLg2 in the ER, we examined the proteolytic cleavage of KDEL-tagged DNLg2. KDEL plays important roles in the localization of many proteins in the ER (Stornaiuolo et al., 2003). This signal determines retrieval from post-ER located compartments in the exocytic pathway by virtue of retrograde transport (Stornaiuolo et al., 2003). We generated four types of reconstructed DNLg2 (Supplementary Figure S2A) and found that types 1 and 2 could not be cleaved whereas types 3 and 4 could (Supplementary Figure S2B). Because the transmembrane domain was removed in types 1 and 2 but kept in types 3 and 4, we concluded that the transmembrane domain is critical in the cleavage process of DNLg2. The KDEL-tagged DNLg2 proteins could also be cleaved, confirming that the cleavage of DNLg2 is achieved in the ER (Supplementary Figure S2B).

Limited trypsin digestion has been used to study protein folding (Gong et al., 2006; De Jaco et al., 2010), because Immature proteins are more sensitive to trypsin digestion. To determine differences between the 130 kDa DNLg2 and the 70 kDa DNLg2, we performed a trypsin digestion experiment. DNLg2 proteins were overexpressed and immunoprecipitated, followed by treatment with limited trypsin. At a trypsin concentration of 2.5  $\mu$ g/ml, the extent of protein degradation was analyzed over 1, 3, 6, or 10 min (Figure 2C). Immunoblotting results showed that levels of the 130 kDa DNLg2 were continuously reduced from 1 min to 10 min, nearly all proteins degraded after 10 min (Figure 2C). In contrast, no changes were observed in the 70 kDa DNLg2 levels (Figure 2C). Parallel treatment without trypsin showed no protein degradation for both 130 kDa and 70 kDa DNLg2 (Figure 2C). This suggests that the 130 kDa DNLg2 is immature, located in the ER, and needs to be cleaved.

#### *Y642–T698 region is required for DNLg2 cleavage*

To elucidate the physiological significance of DNLg2 cleavage, we mapped the proteolytic cleavage site by mutational analysis. Based on the molecular weight of the CTF, the regions around A611 of DNLg2 were predicted to be the candidate site for cleavage (Figure 3A). Therefore, DNLg2 variants with 50 or 100 amino acid deletion around A611 were constructed (named  $\Delta$ 1,  $\Delta$ 2,  $\Delta$ 3,  $\Delta$ 4, or  $\Delta$ 5) and then transfected into S2 cells (Figure 3A). No obvious effects were observed in  $\Delta$ 1 or  $\Delta$ 5 mutant constructs, suggesting that these regions are not necessary for DNLg2 cleavage (Figure 3B). Less amount of the 70 kDa DNLg2 was detected in  $\Delta$ 2 variant, indicating that this region partially contributes to the efficiency of DNLg2 cleavage, but the cleavage site is still beyond this region (Figure 3B). Interestingly, only full-length but not the 70 kDa DNLg2 could be observed in both  $\Delta$ 3 and  $\Delta$ 4 variants (Figure 3B). Thus, the overlap sequences between  $\Delta$ 3 and  $\Delta$ 4 (V649–P704) seemed to be required for the cleavage of DNLg2.

To further narrow down the essential region for cleavage, we generated another series of DNLg2 variants with 11 or 15 amino acid deletion within V649–P704 (named  $\Delta$ 6,  $\Delta$ 7,  $\Delta$ 8, or  $\Delta$ 9) (Figure 3A). Surprisingly, in all of these four variants, only full-length but not the cleaved 70 kDa DNLg2 could be detected (Figure 3C). These results further demonstrated that the overlap

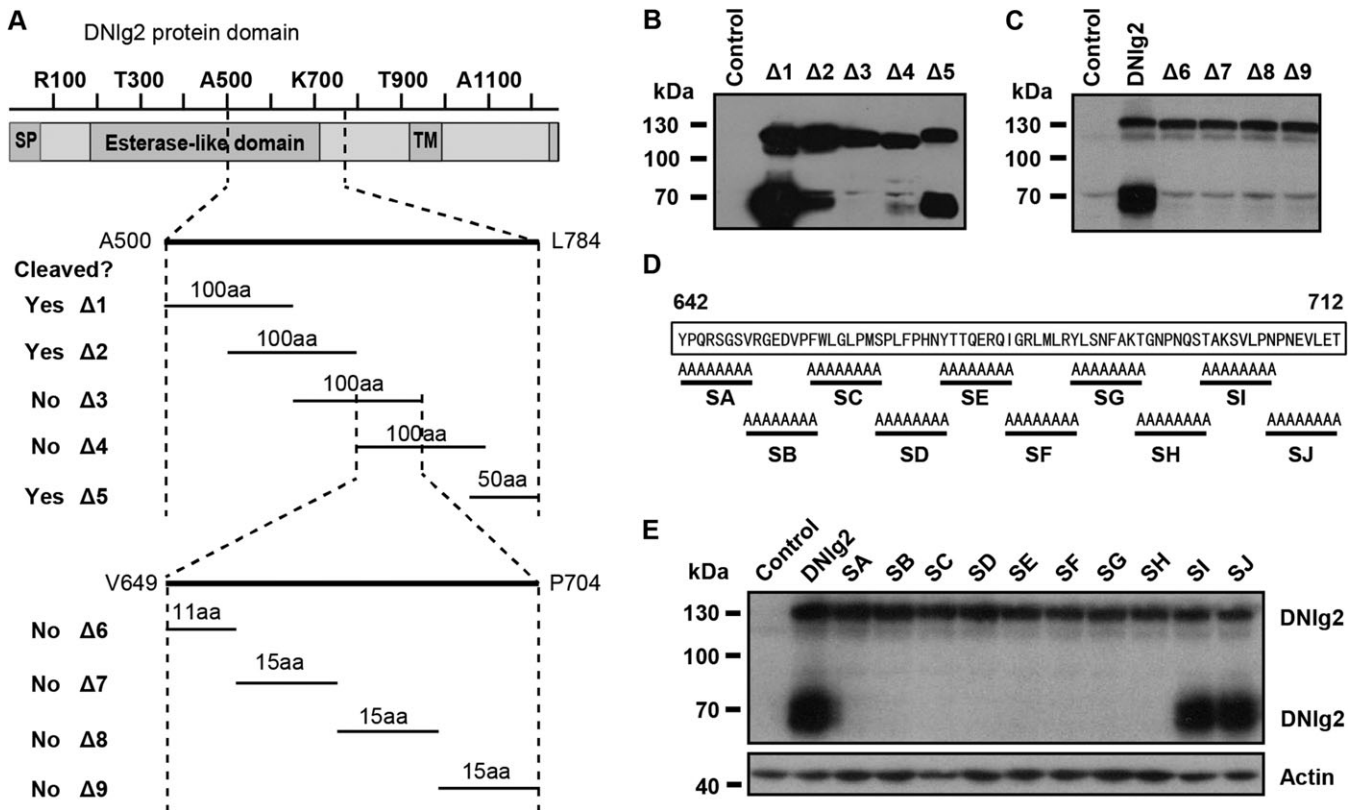


**Figure 3** Y642–T698 region is required for DNlg2 cleavage. **(A)** Schematic diagram of DNlg2 structure. Positions of representative amino acids are shown above. Amino acid lengths and positions of deleted DNlg2 fragments are shown below ( $\Delta 1$ : A500–D599,  $\Delta 2$ : F550–V649,  $\Delta 3$ : A600–A699,  $\Delta 4$ : A650–E749,  $\Delta 5$ : N734–L784,  $\Delta 6$ : V649–G659,  $\Delta 7$ : L660–E674,  $\Delta 8$ : R675–A689, and  $\Delta 9$ : K690–P704). **(B)** Immunoblotting analysis of S2 cells transfected with large deleted DNlg2 fractions. **(C)** Immunoblotting analysis of S2 cells transfected with small deleted DNlg2 sequences. **(D)** Schematic depiction of protein sequences of alanine substitution mutant DNlg2. **(E)** Immunoblotting analysis of S2 cells transfected with alanine substitution mutant DNlg2 constructs. The rabbit anti-DNlg2<sup>CTF</sup> antibodies were used in **B**, **C**, and **E**.

sequences between  $\Delta 3$  and  $\Delta 4$  (V649–P704) are critical for DNlg2 cleavage. These results also indicate that the cleavage of DNlg2 is determined by a large fragment rather than several amino acids.

Another way to identify the functional region is to perform an amino acid substitution assay. Because of the smaller size, no functional group, and smallest effects on the original protein, alanine is widely chosen to substitute amino acids in a protein, such as in the study of Nlg1 cleavage (Suzuki et al., 2012). We then constructed a series of alanine substitutions within DNlg2 and named them SA, SB, SC, SD, SE, SF, SG, SH, SI, or SJ, respectively (Figure 3D). Only SI and SJ were cleaved, while all other mutations inhibited DNlg2 proteolytic cleavage (Figure 3E). Taken together, these data suggest that the region between Y642 and T698 is critical for the proteolytic cleavage of DNlg2 and the cleavage site is located in this region.

#### Autism-associated R598C mutation prevents the cleavage of DNlg2

*In vitro* studies showed that autism-associated R451C mutation in NLG3 resulted in defects in the localization of NLG3 at the cell membrane (Comoletti et al., 2004). We were, therefore, interested in determining whether this mutation leads to

perturbed protein trafficking in DNlg2. By aligning the amino acid sequences of Nlgs among human, mouse, and *Drosophila*, we found that DNlg2 R598 is homologous with Nlg3 R451 (Figure 4A). This arginine is identical in all Nlgs, suggesting its critical and conserved roles in Nlg function (Figure 4A).

To study the effect of the R451C mutation on DNlg2, a site-directed *UAS-dnlg2*<sup>R598C</sup> transgene, which has the same chromosome insertion site with *UAS-dnlg2*, was generated. We used *elav-Gal4* to drive the expression of *UAS-dnlg2* and *UAS-dnlg2*<sup>R598C</sup> in the nervous system, and then performed immunostaining with anti-DNlg2 (6D5) and anti-DVGLUT (synaptic marker) (Daniels et al., 2008). *elav-Gal4* > *UAS-dnlg2*<sup>R598C</sup> flies displayed an abnormal distribution with high levels of DNlg2 in soma and low levels at synaptic regions, compared with *elav-Gal4* > *UAS-dnlg2* (synaptic: 100%  $\pm$  5.3% in *elav-Gal4* > *UAS-dnlg2* vs. 52.8%  $\pm$  2.3% in *elav-Gal4* > *UAS-dnlg2*<sup>R598C</sup>; soma: 100%  $\pm$  5.1% in *elav-Gal4* > *UAS-dnlg2* vs. 190.2%  $\pm$  3.5% in *elav-Gal4* > *UAS-dnlg2*<sup>R598C</sup>) (Figure 4B–D). These observations indicate that the R598C mutation prevents the delivery of DNlg2 from cell bodies to synapses.

Furthermore, immunoblotting results showed that both 130 kDa and 70 kDa bands could be detected when *UAS-dnlg2*

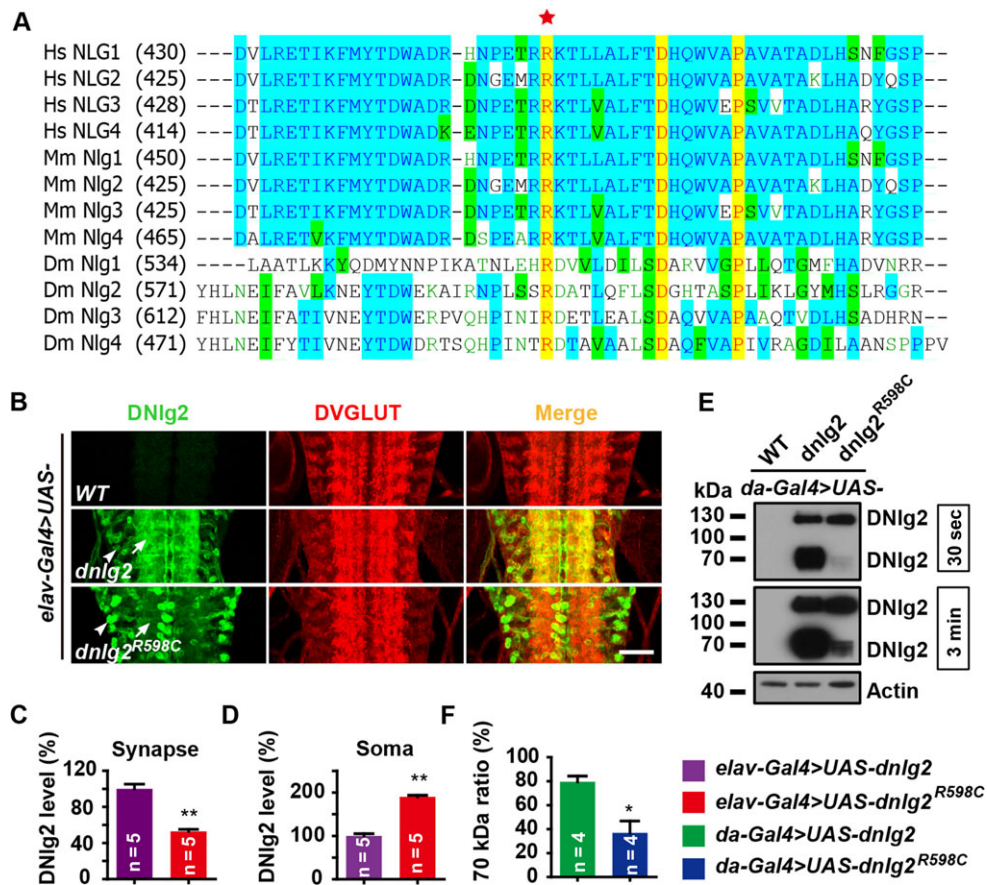


**Figure 4** R598C mutant DNlg2 shows abnormal proteolytic cleavage and trafficking. (A) Multiple sequence alignment of *Homo sapiens* (Hs), *Mus musculus* (Ms), and *Drosophila melanogaster* (Dm) Nlgs. Red star points at the Hs NLG3 R541 amino acid. Hs NLG1 (NP\_055747.1), Hs NLG 2 (NP\_065846), Hs NLG 3 (NP\_061850), Hs NLG 4 (NP\_065793.1), Mm Nlg1 (NP\_619607.2), Mm Nlg2 (NP\_942562.2), Mm Nlg3 (NP\_766520.2), Mm Nlg4 (ABS19580), Dm Nlg1 (NP\_731172), Dm Nlg2 (NP\_523496.1), Dm Nlg3 (NP\_001036685.2), and Dm Nlg4 (NP\_001163661.1). (B) Confocal images of larval brains stained with mouse anti-DNlg2<sup>6D5</sup> (green) and rabbit anti-DVGLUT (red). Genotypes were WT, *elav-Gal4 > UAS-dnlg2*, and *elav-Gal4 > UAS-dnlg2<sup>R598C</sup>*. Scale bar, 50  $\mu$ m. Arrows point at synapse area and arrowheads point at soma site. (C) Quantification of relative DNlg2 protein amount on synapse of each genotype. (D) Quantification of relative DNlg2 protein amount in soma of each genotype. (E) Immunoblotting analysis of DNlg2 in third instar larval muscle cells with shorter (30 sec) and longer (3 min) exposure time. Genotypes were *da-Gal4 > WT*, *da-Gal4 > UAS-dnlg2*, and *da-Gal4 > UAS-dnlg2<sup>R598C</sup>*. The rabbit anti-DNlg2<sup>CTF</sup> antibodies were used. (F) Quantification of the 70 kDa DNlg2 proportion in total proteins. Error bar indicates SEM. \*\* $P < 0.01$ , \* $P < 0.05$ .

and *UAS-dnlg2<sup>R598C</sup>* were overexpressed by *da-Gal4* (Figure 4E). However, in *da-Gal4 > UAS-dnlg2<sup>R598C</sup>* flies, we observed a predominant 130 kDa band, and only upon longer exposure (3 min), a faint 70 kDa band was visible. Inversely, the 70 kDa band was predominant in *da-Gal4 > UAS-dnlg2* transgenic flies (Figure 4E). The proportion of the 70 kDa DNlg2 in total DNlg2 proteins was severely reduced in *da-Gal4 > UAS-dnlg2<sup>R598C</sup>* flies ( $80\% \pm 4.8\%$  in *da-Gal4 > UAS-dnlg2* vs.  $37\% \pm 10.0\%$  in *da-Gal4 > UAS-dnlg2<sup>R598C</sup>*) (Figure 4F). These results demonstrated that the R598C mutation dramatically precludes DNlg2 cleavage.

#### Non-cleavable mutations of DNlg2 block its synapse transport

As R598C mutant DNlg2 exhibited severe defects in proteolytic cleavage and retention in neuron cell bodies, we hypothesized that proteolytic cleavage may be required for the

trafficking of DNlg2. Our biochemical data that the 130 kDa DNlg2 proteins are co-fractionated with the ER protein BiP support this idea. To further confirm this hypothesis *in vivo*, we generated *UAS-dnlg2<sup>SF</sup>* (SF is the alanine substitutional mutation illustrated in Figure 3D) and *UAS-dnlg2<sup>CTF</sup>* (deletion of the Q37–Y684 region) transgenes in the same chromosome insertion site with *UAS-dnlg2* and *UAS-dnlg2<sup>R598C</sup>* (Figure 5A). Immunoblotting analysis showed the presence of only the 130 kDa DNlg2 in *da-Gal4 > UAS-DNlg2<sup>SF</sup>* (Figure 5B). The *da-Gal4 > UAS-dnlg2<sup>CTF</sup>* transgene successfully expressed a DNlg2 fragment lacking partial N-terminal sequence to mimic a cleaved DNlg2 with an obvious 70 kDa band (Figure 5B).

To obtain the precise and clear localization of DNlg2, we took advantage of PDF neurons, which have large and abundant dendritic regions in adult fly brains (Li et al., 2013).

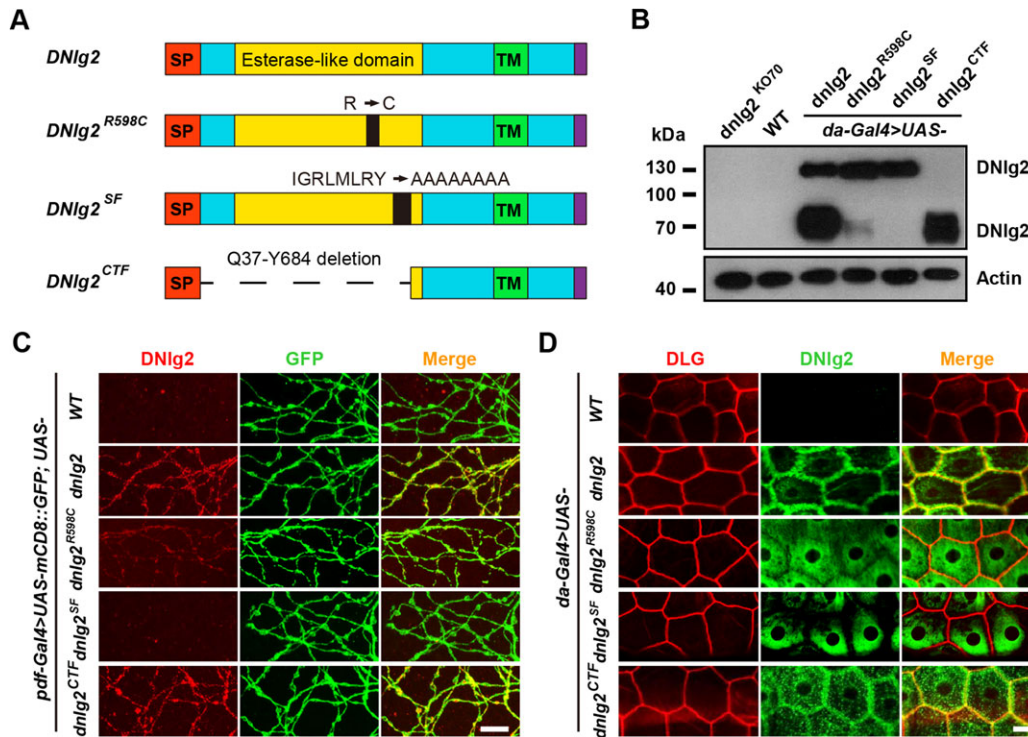


**Figure 5** CTF but not non-cleavable mutant DNlg2 is transported to dendrites or cell surfaces. **(A)** Schematic representation of mutant or N-terminal deleted DNlg2. **(B)** Immunoblotting analysis of *dnlg2* mutant, WT, and *UAS-dnlg2*, *UAS-dnlg2*<sup>R598C</sup>, *UAS-dnlg2*<sup>SF</sup>, *UAS-dnlg2*<sup>CTF</sup> flies with *da-Gal4*. Third instar larval muscle cells were used. The rabbit anti-DNlg2<sup>CTF</sup> antibodies were used. **(C)** Confocal images showing DNlg2 distributions in *pdf-Gal4* > WT, *pdf-Gal4* > *UAS-dnlg2*, *pdf-Gal4* > *UAS-dnlg2*<sup>R598C</sup>, *pdf-Gal4* > *UAS-dnlg2*<sup>SF</sup>, and *pdf-Gal4* > *UAS-dnlg2*<sup>CTF</sup> adult brain dendrite region, labeled with mouse anti-DNlg2<sup>6D5</sup> (red) and rabbit anti-GFP (green). Scale bar, 10  $\mu$ m. **(D)** Confocal images showing DNlg2 distributions of *da-Gal4* > WT, *da-Gal4* > *UAS-dnlg2*, *da-Gal4* > *UAS-dnlg2*<sup>R598C</sup>, *da-Gal4* > *UAS-dnlg2*<sup>SF</sup>, and *da-Gal4* > *UAS-dnlg2*<sup>CTF</sup> epithelial cells, labeled with rabbit anti-DNlg2<sup>CTF</sup> (green) and mouse anti-DLG (red). Scale bar, 25  $\mu$ m.

*UAS-dnlg2*, *UAS-dnlg2*<sup>R598C</sup>, *UAS-dnlg2*<sup>SF</sup>, and *UAS-dnlg2*<sup>CTF</sup> were overexpressed in PDF neurons under the control of *pdf-Gal4*, with *UAS-mCD8::GFP* co-expressed to mark the PDF neuron. Immunostaining revealed that DNlg2<sup>SF</sup>, which only exhibits a 130 kDa band, was unable to be delivered to dendritic sites (Figure 5C). Of particular note is the appropriate translocation of *UAS-dnlg2*<sup>CTF</sup> product, which highly suggested the necessity of proteolytic processing for DNlg2 trafficking (Figure 5C). Consistent with our observation that a small portion of DNlg2<sup>R598C</sup> was cleaved, we also observed a weak signal of this mutant in dendritic regions, compared with normal DNlg2 (Figure 5C).

We also investigated whether mutant DNlg2 could be delivered to plasma membrane in non-neuronal cells. Third instar larval epithelial cells were dissected and stained with anti-DNlg2 (CTF, green) and anti-DLG (red). Immunostaining results showed that overexpressed DNlg2 and DNlg2<sup>CTF</sup> could be delivered to cell surface and co-localized with DLG signaling (Figure 5D). However, R598C and SF mutant DNlg2 were accumulated intracellularly (Figure 5D). Together, these observations indicate that non-cleavable DNlg2 is restricted intracellularly and thus cannot be delivered to cell surface or synapse site.

*BiP* interacts with full-length but not cleaved DNlg2 and mediates the ER retention of full-length DNlg2

To illuminate the localization of non-cleavable DNlg2, we next performed double immunostaining experiments. We observed that non-cleavable DNlg2<sup>R598C</sup> and DNlg2<sup>SF</sup> were co-localized with the ER marker BiP (Haas, 1994), suggesting that the 130 kDa DNlg2 proteins were restricted in the ER (Figure 6A). We also observed increased expression levels of BiP in samples overexpressing *da-Gal4* > *UAS-DNlg2*<sup>SF</sup> and *da-Gal4* > *UAS-DNlg2*<sup>R598C</sup> (Figure 6A). BiP is an essential hsp70 resident protein in the ER, involved in polypeptide translocation, protein folding, and presumably protein degradation (Haas, 1994). To determine the role of BiP in DNlg2 cleavage, we compared the protein levels of BiP among different flies. Immunoblotting analysis showed that BiP levels were increased in *da-Gal4* > *UAS-dnlg2* (192%  $\pm$  43.9%), *da-Gal4* > *UAS-dnlg2*<sup>R598C</sup> (251%  $\pm$  48.3%), and *da-Gal4* > *UAS-dnlg2*<sup>SF</sup> (247%  $\pm$  40.7%) samples (Figure 6B and C). We did not observe any changes of BiP levels in *dnlg2*<sup>KO70</sup> mutant (131%  $\pm$  12%), WT (100%  $\pm$  13.8%), and *da-Gal4* > *UAS-dnlg2*<sup>CTF</sup>-overexpressing (127%  $\pm$  44.2%) flies (Figure 6B and C). These results suggested that only accumulation of full-length DNlg2 can increase

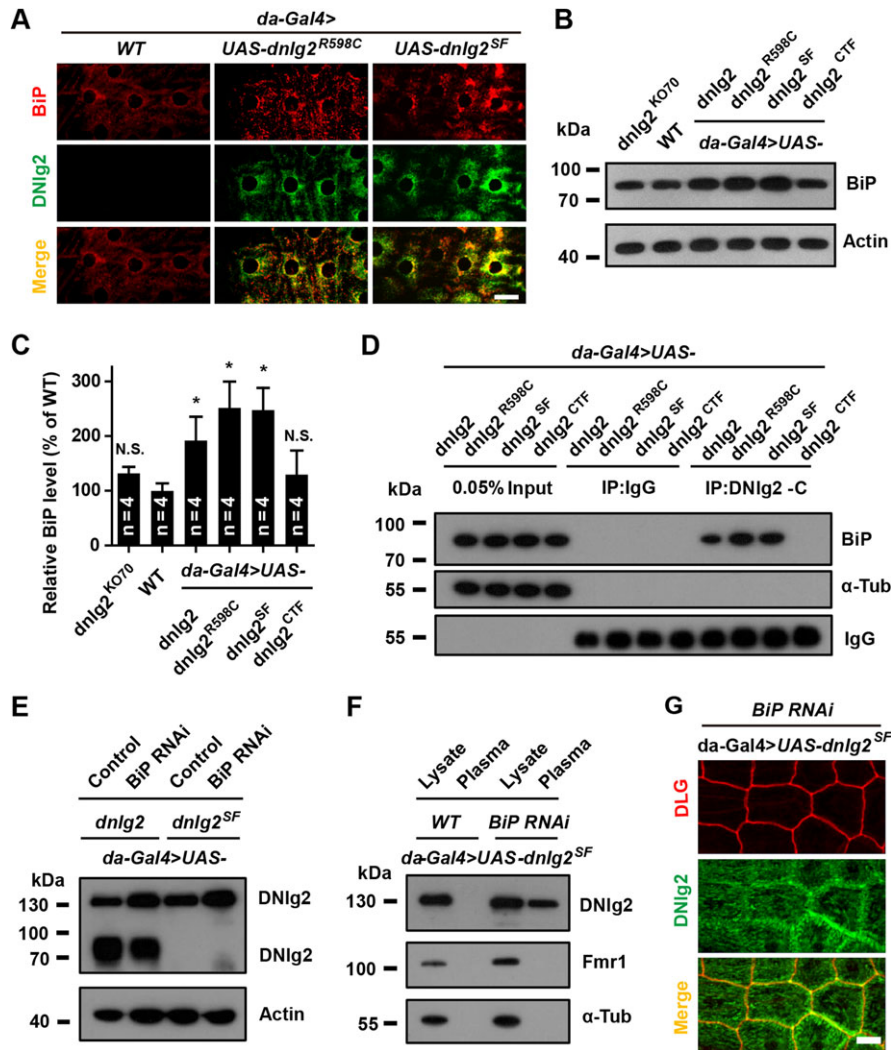


**Figure 6** Full-length DNLg2 is retained in the ER through binding to BiP. **(A)** Confocal images showing non-cleavable DNLg2 (*da-Gal4 > UAS-dnlg2* and *da-Gal4 > UAS-dnlg2<sup>R598C</sup>*) co-localized with BiP. Dissected epithelial cells were co-stained with rabbit anti-DNLg2<sup>CTF</sup> (green) and rat anti-BiP (red, showing the ER). Scale bar, 25  $\mu$ m. **(B)** Immunoblotting analysis of *dnlg2* mutant, WT, and *da-Gal4 > UAS-dnlg2*, *da-Gal4 > UAS-dnlg2<sup>R598C</sup>*, *da-Gal4 > UAS-dnlg2<sup>SF</sup>*, *da-Gal4 > UAS-dnlg2<sup>CTF</sup>* flies with anti-BiP. **(C)** Quantification of relative BiP expression level in each genotype. **(D)** Co-immunoprecipitation of DNLg2 and BiP *in vivo*. **(E)** Immunoblotting analysis of *da-Gal4* overexpressing *UAS-dnlg2* and *UAS-dnlg2<sup>SF</sup>* at WT or BiP RNAi background with rabbit anti-DNLg2<sup>CTF</sup>. **(F)** Immunoblotting analysis of *da-Gal4 > UAS-dnlg2<sup>SF</sup>* and *da-Gal4 > UAS-BiP-RNAi, UAS-dnlg2<sup>SF</sup>* with rabbit anti-DNLg2<sup>CTF</sup>. Samples were purified with plasma-membrane extraction kit. **(G)** Confocal images of *UAS-dnlg2<sup>SF</sup>*-overexpressing flies under BiP knockdown background with *da-Gal4*. Dissected epithelial cells were co-stained with rabbit anti-DNLg2<sup>CTF</sup> (green) and mouse anti-DLG antibody (red). Scale bar, 20  $\mu$ m.

BiP expression levels. In addition, co-immunoprecipitation experiments confirmed an *in vivo* interaction between BiP and the 130 kDa DNLg2 rather than 70 kDa DNLg2<sup>CTF</sup> fragment (Figure 6D), demonstrating that BiP associates with the 130 kDa DNLg2 rather than the 70 kDa DNLg2.

We, therefore, speculated that such association may be responsible for the ER retention of the 130 kDa DNLg2. To confirm this hypothesis, we analyzed the effects of BiP knockdown on DNLg2 proteins by using *da-Gal4 > UAS-BiP-RNAi* flies, where BiP expression level was decreased (Supplementary Figure S3A and B). The expression level of the 70 kDa DNLg2 was decreased,

while the 130 kDa DNLg2 was increased in *da-Gal4 > UAS-dnlg2*, *UAS-BiP-RNAi* flies (Figure 6E). The expression level of DNLg2<sup>SF</sup> proteins was also increased in *da-Gal4 > UAS-dnlg2<sup>SF</sup>*, *UAS-BiP-RNAi* flies (Figure 6E). These results indicate that BiP is involved in the maturation and degradation of the 130 kDa DNLg2.

Furthermore, we purified the plasma membrane proteins from *da-Gal4 > UAS-dnlg2<sup>SF</sup>* or *da-Gal4 > UAS-dnlg2<sup>SF</sup>, UAS-BiP-RNAi* flies. Immunoblotting results showed that in *da-Gal4 > UAS-dnlg2<sup>SF</sup>* flies, DNLg2<sup>SF</sup> proteins could not be detected in purified plasma membrane fractions (Figure 6F). Intriguingly, a small portion of DNLg2<sup>SF</sup> proteins appeared in purified plasma membrane

fractions from BiP RNAi flies (Figure 6F). Here, we used Fmr1 and  $\alpha$ -Tubulin as negative controls, which could not be detected in plasma membrane fractions (Figure 6F). Similarly, a small portion of the 130 kDa DNLg2 could be detected in plasma membrane fractions from *da-Gal4 > UAS-dnlg2*, *UAS-BiP-RNAi* flies (Supplementary Figure S3C and D). In addition, the third instar larval epithelial cells of *da-Gal4 > UAS-dnlg2<sup>SF</sup>*, *UAS-BiP-RNAi* flies were dissected and stained with anti-DNLg2 (6D5, green) and anti-DLG (red). Immunostaining results showed that the 130 kDa DNLg2<sup>SF</sup> proteins co-localized with DLG at epithelial cell surface in *da-Gal4 > UAS-dnlg2<sup>SF</sup>*, *UAS-BiP-RNAi* flies (Figure 6G), indicating that the 130 kDa DNLg2 proteins might escape to the cell surface when the amount of BiP proteins are insufficient. Taken together, we demonstrated that BiP mediates full-length DNLg2 protein maturation and rigorously restricts full-length DNLg2 proteins in the ER, which plays vital roles in the maturation and cleavage of DNLg2.

#### *DNLg2 CTF can rescue defective neuromuscular junction growth in dnlg2 mutant flies*

As the 130 kDa DNLg2 is restricted in the ER, it is easy to speculate that the 70 kDa DNLg2 is the functional isoform. It has been previously reported that DNLg2 is required for synapse development and function at the neuromuscular junction (NMJ). In the rescue experiments, our observations were consistent with previous data showing that the total number of boutons were significantly reduced in the *dnlg2* mutants compared with WT controls (100%  $\pm$  3.1% in WT vs. 62.9%  $\pm$  10.7% in *dnlg2<sup>K070</sup>*) (Figure 7A and B). These changes could be rescued with ubiquitous expression of *UAS-dnlg2* (107%  $\pm$  5.0%) or *UAS-dnlg2<sup>CTF</sup>* (101.7%  $\pm$  3.7%) driven by *da-Gal4* (Figure 7A and B). However, ubiquitous expression of *UAS-dnlg2<sup>R598C</sup>* (65.8%  $\pm$  3.9%) or *UAS-dnlg2<sup>SF</sup>* (54.4%  $\pm$  4.7%) driven by *da-Gal4* could not rescue the reduced bouton numbers (Figure 7A and B). These results suggest that the 70 kDa but not 130 kDa DNLg2 is functional.

In addition, we found that the postsynaptic GluRIIB signal was markedly reduced in *dnlg2* mutants compared with WT controls, which could also be restored through ubiquitous expression of *UAS-dnlg2* (113.4%  $\pm$  12.6%) or *UAS-dnlg2<sup>CTF</sup>* (102.1%  $\pm$  10.2%) (Figure 7C and D). In contrast, *UAS-dnlg2<sup>SF</sup>* (61.5%  $\pm$  12.6%) was unable to restore defective GluRIIB phenotypes, suggesting that non-cleavable DNLg2 is non-functional (Figure 7C and D). Intriguingly, *UAS-dnlg2<sup>R598C</sup>* (98.4%  $\pm$  6.0%) rescued the defects in GluRIIB levels (Figure 7C and D). This might be arising from the small portion of cleaved 70 kDa DNLg2 in *UAS-dnlg2<sup>R598C</sup>* flies.

Moreover, electrophysiology experiments with the rescue lines at the NMJ showed that non-cleavable DNLg2 could not rescue the reduced synaptic transmission in *dnlg2* mutants (Supplementary Figure S4A–D). Overall, these findings indicate that the 70 kDa DNLg2 proteins derived from the proteolytic cleavage reaction promote *Drosophila* NMJ development.

#### Discussion

It is well known that proteolytic cleavage plays critical roles in numerous biological processes such as development, differentiation, and cell migration. The cleavages of synapse adhesive

molecules usually occur on the synapse in neuronal activity-dependent manner (Conant et al., 2015). Mouse Nlg1 proteolytic processing belongs to this type of neuronal activity-dependent event (Peixoto et al., 2012). The potential proteolytic cleavages were observed in DNLg2 (Sun et al., 2011) and DNLg3 (Xing et al., 2014) too. However, their mechanisms and functions had yet to be investigated.

In this study, we have revealed a quite different proteolytic processing event and provided compelling support for a novel hypothesis where, in contrast to the activity-dependent cleavage of Nlg1 on the synapse in rodents, the cleavage of DNLg2 is achieved in the ER and the cleaved 70 kDa DNLg2 is the functional isoform. In other words, the emerging model we present in this work suggests that the cleavage of DNLg2 in the ER is a requirement for its trafficking and function. Importantly, given that overexpression of autism-associated R598C mutation precludes the cleavage of DNLg2, which may be one of the potential autism pathogenesis, our study provides the first link among autism-associated mutation, proteolytic cleavage, and the trafficking of Nlgs. Thus, these findings provide a new insight in understanding the complicated regulatory mechanisms of Nlg maturation and trafficking in synapse development and function.

Nlgs were identified in different species from *C. elegans* to Human, including four homologs in mammals, plus an additional homolog on the Y chromosome in humans, and four homologs in *Drosophila* (Knight et al., 2011). However, due to diversifying independently during evolution, the name orders of DNLg1–4 are not in correspondence to mammal Nlg1–4, respectively (Knight et al., 2011).

Here, we found that the cleavage of DNLg2 is a novel mechanism underlying Nlg maturation and function, which is quite different from mammal Nlg1 cleavage. First, the cleavage of DNLg2 is continuous and ubiquitous but not activity dependent, suggesting that the cleavage modification plays critical roles in DNLg2 maturation. Second, the cleavage event is achieved in the ER but not on the cell surface, and is required for DNLg2 ER export. The finding that the endogenous full-length DNLg2 is only detected in the ER fractions strongly supports these conclusions. Finally, the cleavage efficiency of DNLg2 is extremely high. In WT mice, both full-length and cleaved CTF of Nlg1 proteins can be easily detected, and the expression levels of the two bands are similar (Suzuki et al., 2012). Such phenomenon is also observed for DNLg3 in WT flies (Xing et al., 2014). However, most of the full-length DNLg2 proteins were cleaved into 70 kDa. The different proteolytic cleavage mechanisms of DNLg2 and mammal Nlg1 suggest a variety of potential regulation manners for Nlg cleavage. As Nlgs are highly conserved, it would be interesting to determine in the future whether the DNLg2 cleavage mechanisms also exist in one of the undetermined mammal Nlgs.

Analyses on density gradient separation fractions demonstrate that the 130 kDa DNLg2 only exits in ER, while the 70 kDa DNLg2 exits in both ER and Golgi. By characterizing a variety of mutant transgenic flies, we also demonstrate that non-cleavable DNLg2 is restricted in the ER and is non-functional. The 130 kDa

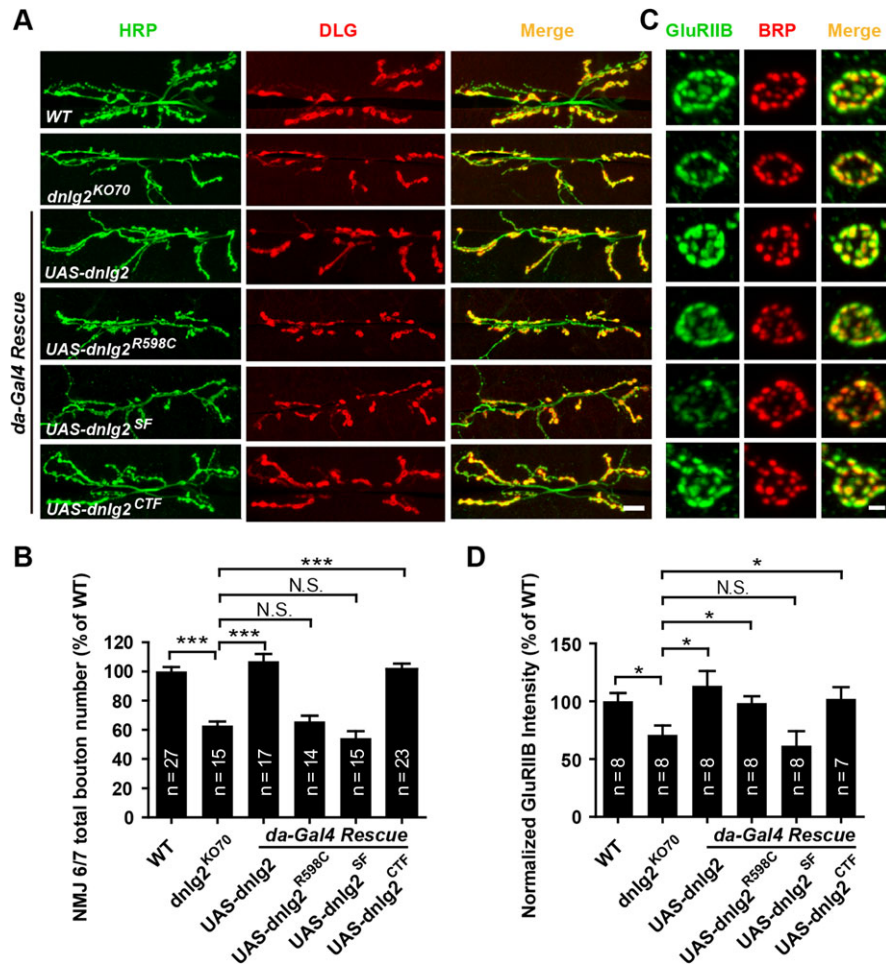


**Figure 7** The 70 kDa DNLg2 promotes NMJ development. **(A)** Confocal images of NMJ6/7 from abdominal segment 2 of third instar larvae labeled with rabbit anti-HRP (green) and mouse anti-DLG (red), showing bouton phenotypes in WT, *dnlg2*<sup>KO70</sup>, and rescue lines with UAS-*dnlg2*, UAS-*dnlg2*<sup>R598C</sup>, UAS-*dnlg2*<sup>SF</sup>, UAS-*dnlg2*<sup>CTF</sup> derived by *da-Gal4*. Scale bar, 25  $\mu$ m. **(B)** Quantification of total bouton number at NMJ6/7, adjusted to WT bouton number. **(C)** Confocal images of synaptic boutons at NMJ4 labeled with rabbit anti-GluRIIB (green) and mouse anti-BRP (red), showing GluRIIB signal phenotypes in WT, *dnlg2*<sup>KO70</sup>, and rescue lines with UAS-*dnlg2*, UAS-*dnlg2*<sup>R598C</sup>, UAS-*dnlg2*<sup>SF</sup>, UAS-*dnlg2*<sup>CTF</sup> derived by *da-Gal4*. Scale bar, 5  $\mu$ m. **(D)** Quantification of GluRIIB signal intensity with 3D reconstructed confocal images.

DNLg2 seems to be precursor immature proteins, for it is more sensitive to limited trypsin digestion. These results support the idea that the 130 kDa DNLg2 is restricted in the ER and cannot be delivered to the Golgi, and the proteolytic cleavage activates DNLg2.

Newly translated membrane proteins enter the ER in an unfolded state (Rapoport, 2007), whereby chaperones and enzymes regulate their folding and maturation (Ruggiano et al., 2014). Here, the ER chaperone BiP can selectively interact with the 130 kDa DNLg2, rather than the 70 kDa DNLg2, for the maturation control of DNLg2. When BiP is knocked down, the ER restricted 130 kDa DNLg2 proteins can escape to the cell surface. Genetic analysis showed that these escaped 130 kDa DNLg2<sup>SF</sup> might be still non-functional (Supplementary Figure S5A and B). The 130 kDa DNLg2 proteins associate with BiP until they turn into 70 kDa; otherwise, they will be degraded with the help of BiP. Our findings are consistent with previous data showing altered interactions of the mutant

Nlgs with chaperones in the ER and arrest of transport along the secretory pathway with diversion to the proteasome (De Jaco et al., 2010). This may explain why the total expression levels of DNLg2<sup>R598C</sup> or DNLg2<sup>SF</sup> are much less than WT DNLg2 when they are overexpressed both *in vivo* and *in vitro*. These results indicate that BiP-involving cleavage may play important roles in the quality and quantity control of DNLg2. The expression levels of Nlgs are thought to be related with their physiological and pathological functions, which regulate the number and ratio of NMDA/AMPA receptors of the synapses (Chubykin et al., 2007). This may be the physiological reason why the 130 kDa DNLg2 has to be cleaved in the ER.

Usually, the level of the 130 kDa DNLg2 is quite low, while the level of the 70 kDa DNLg2 is very high. According to our findings, this is because the 130 kDa DNLg2 proteins are immature proteins and are cleaved into the 70 kDa isoform in the ER continuously. Therefore, we speculated that the 70 kDa DNLg2

proteins are functional. The rescue experiments showing that the 70 kDa DNLg2 can restore bouton development and GluRIIB defects support our hypothesis. This is also consistent with previous data showing that overexpression of Nlg1-CTF that lacks the extracellular domain retained the capacity to induce dendritic spines in granule cells (Suzuki et al., 2012), and that cytoplasmic domain of Nlg1 is necessary and sufficient for the induction of dendritic spines in transfected neurons (Ko et al., 2009). On the other hand, overexpressed 70 kDa DNLg2 may promote postsynaptic overgrowth, and thus compensate for the function of DNLg2-NTF. It is intriguing to determine whether the NTF contributes to synapse function or other neurological significances in the future.

Multiple independent mutations in Nlgs were identified in patients with autism, and most of the mutations localize to the  $\alpha/\beta$  hydrolase fold domain of Nlgs, resulting in a loss of protein function. Of note is the R451C mutation in human NLG3 (Jamain et al., 2003; Comoletti et al., 2004). This arginine is identical in all Nlgs, suggesting a critical role of this amino acid residue. Previous results show that these mutations in Nlgs impact their trafficking (Comoletti et al., 2004; Zhang et al., 2009; De Jaco et al., 2010). However, it is remaining unknown whether these mutations affect the cleavage of Nlgs until now. Interestingly, the homology R598C mutation in DNLg2 affects the proteolytic cleavage and trafficking, leading to retention of DNLg2 in the ER. The similar trafficking defects observed in humans and *Drosophila* suggest that this autism-associated mutation has conserved effects, which might also affect NLG proteolytic cleavage in humans. Therefore, it is tempting to speculate that abnormalities in the proteolytic processing of NLGs may be involved in the pathology of the neurodevelopmental diseases.

To the best of our knowledge, this study provides the first known link between the autism-associated mutation and proteolytic cleavage in Nlgs. People started to realize the cleavage modification to Nlgs from the year 2012, and only mouse/rat Nlg1 cleavage has been analyzed (Peixoto et al., 2012; Suzuki et al., 2012). Therefore, it is urgent to study the cleavage of mammal Nlg2, Nlg3, or Nlg4 and determine the cleavage of Nlgs in autism patients in the future.

It is interesting that the R598 is beyond the cleavage region Y642–T698 but its mutation still affects DNLg2 cleavage. Our mutational analyses indicate that a large region is required in DNLg2 cleavage reaction, and the proper structure and conformation, but not several amino acids, are crucial for the cleavage. Therefore, the R598C mutation may break the conformation instead of directly affecting cleavage site.

Finally, identification of responsible protease(s) and relevant auxiliary components in the ER would provide important information on the proteolytic control of Nlgs. It would be interesting to identify the protease(s) involved in DNLg2 cleavage in the future.

## Materials and methods

### Fly stocks

Flies were raised at 25°C (except those used in the *Gal4/Tub-Gal80<sup>ts</sup>* experiments) with a 12-h light/dark cycle on standard

medium. The WT fly strain used in this study was *w<sup>1118</sup>. elav-Gal4, C57-Gal4, pdf-Gal4, gmr-Gal4, repo-Gal4, da-Gal4*, and *attP* transgenic flies (35568) were obtained from the *Drosophila* Stock Center (Bloomington). BiP RNAi line (THU0848) was obtained from the Tsinghua Fly Center.

More detailed experimental procedures are described in Supplementary material.

## Supplementary material

Supplementary material is available at *Journal of Molecular Cell Biology* online.

## Acknowledgements

We thank Dr Chengqi Lin (Southeast University), Dr Gabrielle L. Boulianne (University of Toronto), and Dr Zhengping Jia (University of Toronto) for useful discussions and critical comments on the manuscript, the Bloomington Stock Center and Tsinghua Fly Center for providing *Drosophila* stocks, DSHB for antibodies, and the members of the Xie laboratory for their critical comments on the manuscript.

## Funding

This work was supported by grants from the National Natural Science Foundation of China (31430035 and 31171041) and the National Basic Research Program of China (973 Program, 2012CB517903 to W.X.).

**Conflict of interest:** none declared.

## References

- Banovic, D., Khorramshahi, O., Oswald, D., et al. (2010). *Drosophila* neuroligin 1 promotes growth and postsynaptic differentiation at glutamatergic neuromuscular junctions. *Neuron* 66, 724–738.
- Bischof, J., Maeda, R.K., Hediger, M., et al. (2007). An optimized transgenesis system for *Drosophila* using germ-line-specific phiC31 integrases. *Proc. Natl Acad. Sci. USA* 104, 3312–3317.
- Chubykin, A.A., Atasoy, D., Etherton, M.R., et al. (2007). Activity-dependent validation of excitatory versus inhibitory synapses by neuroligin-1 versus neuroligin-2. *Neuron* 54, 919–931.
- Comoletti, D., De Jaco, A., Jennings, L.L., et al. (2004). The Arg451Cys-neuroligin-3 mutation associated with autism reveals a defect in protein processing. *J. Neurosci.* 24, 4889–4893.
- Conant, K., Allen, M., and Lim, S.T. (2015). Activity dependent CAM cleavage and neurotransmission. *Front. Cell. Neurosci.* 9, 305.
- Daniels, R.W., Gelfand, M.V., Collins, C.A., et al. (2008). Visualizing glutamatergic cell bodies and synapses in *Drosophila* larval and adult CNS. *J. Comp. Neurol.* 508, 131–152.
- De Jaco, A., Lin, M.Z., Dubi, N., et al. (2010). Neuroligin trafficking deficiencies arising from mutations in the  $\alpha/\beta$ -hydrolase fold protein family. *J. Biol. Chem.* 285, 28674–28682.
- Etherton, M., Foldy, C., Sharma, M., et al. (2011). Autism-linked neuroligin-3 R451C mutation differentially alters hippocampal and cortical synaptic function. *Proc. Natl Acad. Sci. USA* 108, 13764–13769.
- Giagtzoglou, N., Ly, C.V., and Bellen, H.J. (2009). Cell adhesion, the backbone of the synapse: ‘vertebrate’ and ‘invertebrate’ perspectives. *Cold Spring Harb. Perspect. Biol.* 1, a003079.
- Gong, Q., Jones, M.A., and Zhou, Z. (2006). Mechanisms of pharmacological rescue of trafficking-defective hERG mutant channels in human long QT syndrome. *J. Biol. Chem.* 281, 4069–4074.

- Haas, I.G. (1994). BiP (GRP78), an essential hsp70 resident protein in the endoplasmic reticulum. *Experientia* 50, 1012–1020.
- Hahn, N., Geurten, B., Gurvich, A., et al. (2013). Monogenic heritable autism gene neuroligin impacts *Drosophila* social behaviour. *Behav. Brain Res.* 252, 450–457.
- Ichtchenko, K., Hata, Y., Nguyen, T., et al. (1995). Neuroligin 1: a splice site-specific ligand for  $\beta$ -neurexins. *Cell* 81, 435–443.
- Irie, M., Hata, Y., Takeuchi, M., et al. (1997). Binding of neuroligins to PSD-95. *Science* 277, 1511–1515.
- Jamain, S., Quach, H., Betancur, C., et al. (2003). Mutations of the X-linked genes encoding neuroligins NLGN3 and NLGN4 are associated with autism. *Nat. Genet.* 34, 27–29.
- Jiang, R. (2015). Walking on multiple disease-gene networks to prioritize candidate genes. *J. Mol. Cell Biol.* 7, 214–230.
- Knight, D., Xie, W., and Boulianne, G.L. (2011). Neurexins and neuroligins: recent insights from invertebrates. *Mol. Neurobiol.* 44, 426–440.
- Ko, J., Zhang, C., Arac, D., et al. (2009). Neuroligin-1 performs neurexin-dependent and neurexin-independent functions in synapse validation. *EMBO. J.* 28, 3244–3255.
- Li, Y., Zhou, Z., Zhang, X., et al. (2013). *Drosophila* neuroligin 4 regulates sleep through modulating GABA transmission. *J. Neurosci.* 33, 15545–15554.
- Lin, H.H., Chang, G.W., Davies, J.Q., et al. (2004). Autocatalytic cleavage of the EMR2 receptor occurs at a conserved G protein-coupled receptor proteolytic site motif. *J. Biol. Chem.* 279, 31823–31832.
- Liu, A., Zhou, Z., Dang, R., et al. (2016). Neuroligin 1 regulates spines and synaptic plasticity via LIMK1/cofilin-mediated actin reorganization. *J. Cell Biol.* 212, 449–463.
- Mozer, B.A., and Sandstrom, D.J. (2012). *Drosophila* neuroligin 1 regulates synaptic growth and function in response to activity and phosphoinositide-3-kinase. *Mol. Cell. Neurosci.* 51, 89–100.
- Peixoto, R.T., Kunz, P.A., Kwon, H., et al. (2012). Transsynaptic signaling by activity-dependent cleavage of neuroligin-1. *Neuron* 76, 396–409.
- Qian, J., Tu, R., Yuan, L., et al. (2016). Intronic miR-932 targets the coding region of its host gene, *Drosophila* neuroligin2. *Exp. Cell Res.* 344, 183–193.
- Rapoport, T.A. (2007). Protein translocation across the eukaryotic endoplasmic reticulum and bacterial plasma membranes. *Nature* 450, 663–669.
- Ruggiano, A., Foresti, O., and Carvalho, P. (2014). Quality control: ER-associated degradation: protein quality control and beyond. *J. Cell Biol.* 204, 869–879.
- Südhof, T.C. (2008). Neuroligins and neurexins link synaptic function to cognitive disease. *Nature* 455, 903–911.
- Stein, D., Charatsi, I., Cho, Y.S., et al. (2010). Localization and activation of the *Drosophila* protease easter require the ER-resident saposin-like protein seele. *Curr. Biol.* 20, 1953–1958.
- Stornauiolo, M., Lotti, L.V., Borgese, N., et al. (2003). KDEL and KKXX retrieval signals appended to the same reporter protein determine different trafficking between endoplasmic reticulum, intermediate compartment, and Golgi complex. *Mol. Biol. Cell* 14, 889–902.
- Sun, M., Xing, G., Yuan, L., et al. (2011). Neuroligin 2 is required for synapse development and function at the *Drosophila* neuromuscular junction. *J. Neurosci.* 31, 687–699.
- Suzuki, K., Hayashi, Y., Nakahara, S., et al. (2012). Activity-dependent proteolytic cleavage of neuroligin-1. *Neuron* 76, 410–422.
- Szatmari, P., Paterson, A.D., Zwaigenbaum, L., et al. (2007). Mapping autism risk loci using genetic linkage and chromosomal rearrangements. *Nat. Genet.* 39, 319–328.
- Ulbrich, L., Favaloro, F.L., Trobiani, L., et al. (2016). Autism-associated R451C mutation in neuroligin3 leads to activation of the unfolded protein response in a PC12 Tet-On inducible system. *Biochem. J.* 473, 423–434.
- Venkatesh, H.S., Johung, T.B., Caretti, V., et al. (2015). Neuronal activity promotes glioma growth through neuroligin-3 secretion. *Cell* 161, 803–816.
- Vogel, J.L., and Kristie, T.M. (2000). Autocatalytic proteolysis of the transcription factor-coactivator C1 (HCF): a potential role for proteolytic regulation of coactivator function. *Proc. Natl Acad. Sci. USA* 97, 9425–9430.
- Xie, J., Jiang, H., Wan, Y.H., et al. (2011). Induction of a 55 kDa acetylcholinesterase protein during apoptosis and its negative regulation by the Akt pathway. *J. Mol. Cell Biol.* 3, 250–259.
- Xing, G., Gan, G., Chen, D., et al. (2014). *Drosophila* neuroligin3 regulates neuromuscular junction development and synaptic differentiation. *J. Biol. Chem.* 289, 31867–31877.
- Xu, H., Boulianne, G.L., and Trimble, W.S. (2002). *Drosophila* syntaxin 16 is a Q-SNARE implicated in Golgi dynamics. *J. Cell Sci.* 115, 4447–4455.
- Zhang, C., Milunsky, J.M., Newton, S., et al. (2009). A neuroligin-4 missense mutation associated with autism impairs neuroligin-4 folding and endoplasmic reticulum export. *J. Neurosci.* 29, 10843–10854.